Encyclopedia of Atmospheric Sciences

Editor-in-Chief

James R. Holton

University of Washington, Seattle, U.S.A.

Editors

John Pyle

University of Cambridge, U.K.

Judith A. Curry

Georgia Institute of Technology, U.S.A.

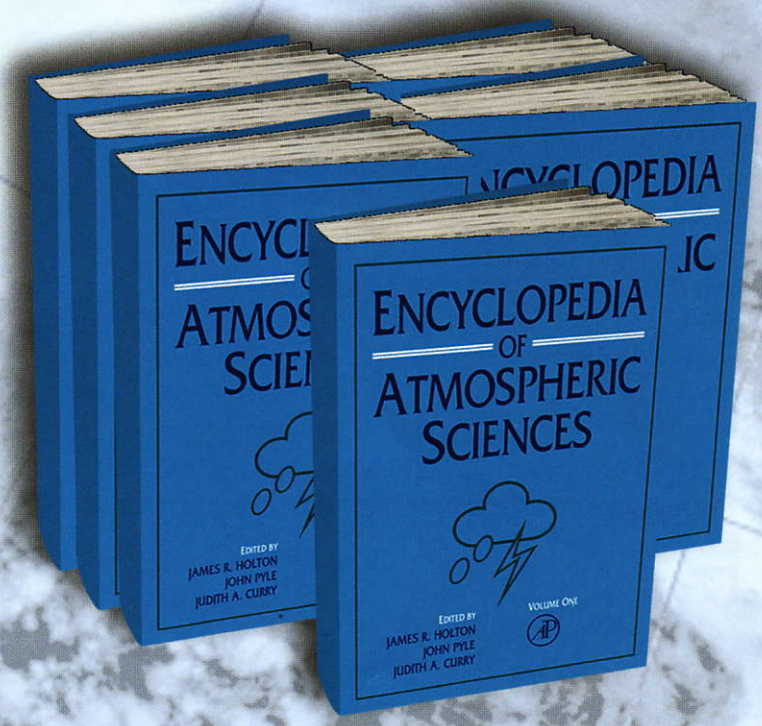

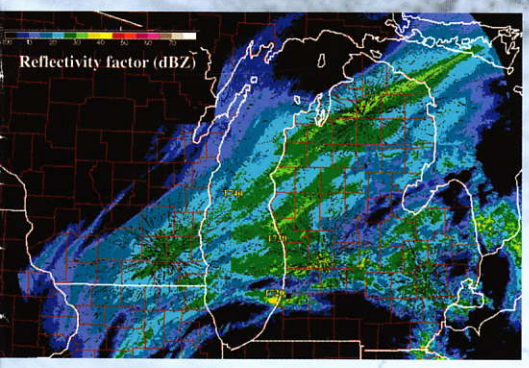

"I greatly welcome this unique Encyclopedia of six volumes containing 340 contributions, each of approximately 4000 words, on all major aspects of atmospheric science and cognate subjects such as oceanography and hydrology, and that range from Acid Rain to the World Climate Research Programme. ... The six volumes promise to be the most comprehensive and widely consulted publication in the atmospheric sciences for years to come. Every scientist engaged in post-graduate teaching and research in the subject will need access to a copy."

—From the Foreword by Sir John Mason, F.R.S., Imperial College, London, U.K.

www.academicpress.com/atmospheric

ACADEMIC PRESS
An imprint of Elsevier Science

STATIONARY WAVES (OROGRAPHIC AND THERMALLY FORCED)

S Nigam, University of Maryland, College Park, MD, USA

E DeWeaver, University of Wisconsin, Madison, WI, USA

Introduction

The term stationary waves refers to the zonally asymmetric features of the time-averaged atmospheric circulation. They are also referred to as standing eddies, where standing refers to the time averaging over a month to season, and eddy is a generic term for zonally asymmetric patterns. The zonal asymmetries of the seasonal circulation are particularly interesting because they occur despite the longitudinally uniform incidence of solar radiation on our planet. Stationary waves must arise, ultimately, due to asymmetries at the Earth's surface – mountains, continent–ocean contrasts, and sea surface temperature asymmetries. Understanding precisely how the stationary waves are generated and maintained is a fundamental problem in climate dynamics.

Stationary waves have a strong effect on the climate through their persistent northerly and southerly surface winds, which blow cold and warm air. Advection of moisture by the stationary wave flow contributes to hydroclimate variations over the continents. Beyond their direct advective impact, stationary waves control the location of stormtracks – the preferred paths of synoptic weather systems in the midlatitudes, and the zone of tropical–extratropical interaction in the subtropics. Stationary waves are important also on longer time scales, since interannual climate variability projects substantially on the zonally asymmetric component of the flow. Finally, stationary waves contribute significantly to the maintenance of the complementary zonally symmetric circulation, in both climatological and anomalous states; the contribution is through quadratic fluxes of meridional momentum and heat. Stationary waves are thus a fundamental feature of the general circulation of the troposphere.

Observed Structure

Stationary waves are stronger in the Northern Hemisphere because of greater orography and continentality. Wave amplitudes in the Northern Hemisphere are largest during winter, modest during the transition seasons of spring and autumn, and weakest during summer. The Southern Hemisphere stationary waves and their seasonal variation are substantially smaller in comparison.

Northern Hemisphere Winter Structure

Because of the geostrophic balance condition, stationary waves in the upper-level flow can be conveniently displayed using the height of the 300 hPa pressure surface. The geostrophic wind blows along the height contours, with lower heights to the left in the Northern Hemisphere, and with a speed proportional to the gradient of the height field. The height of the 300 hPa surface varies considerably with latitude and longitude (**Figure 1A**), with the mean height being close to 9 km. The polar vortex is clearly recognizable in this projection. The vortex is due to insolation and planetary rotation, both zonally symmetric inputs, but the vortex has notable departures from symmetry: troughs over northern Canada and western Siberia, and ridges over the eastern Atlantic and Pacific. (The zonally asymmetric component of the field which highlights the troughs and ridges is shown later, in **Figure 2A**.) The regions where the height contours are close together correspond to strong westerly (coming from the west) jets: the Asian–Pacific and North American jets.

Stationary waves at the Earth's surface can be identified using the sea-level pressure field, which in elevated areas is the surface pressure reduced to sea level. The lightly shaded regions in **Figure 1B** are surface lows, and the dark regions are highs. Lows are found over both ocean basins, the Aleutian Low in the Pacific and the Icelandic Low in the Atlantic. The Aleutian Low is centered off the tip of the Aleutian Islands chain, and the counterclockwise flow around the low brings southerly marine air to coastal Canada and Alaska, lessening the severity of the winter season. To the south of the Icelandic Low is a high-pressure center known as the Azores High. Strong onshore surface flow occurs between the Icelandic Low and the Azores High, again lessening the severity of coastal winters in Europe. Much higher surface pressure can be found over central Asia in a center called the Siberian High. Between the Siberian High and the Aleutian Low is a region of strong northerly flow, which brings down colder air and lowers near-surface temperature along the east coast of Asia. The winter

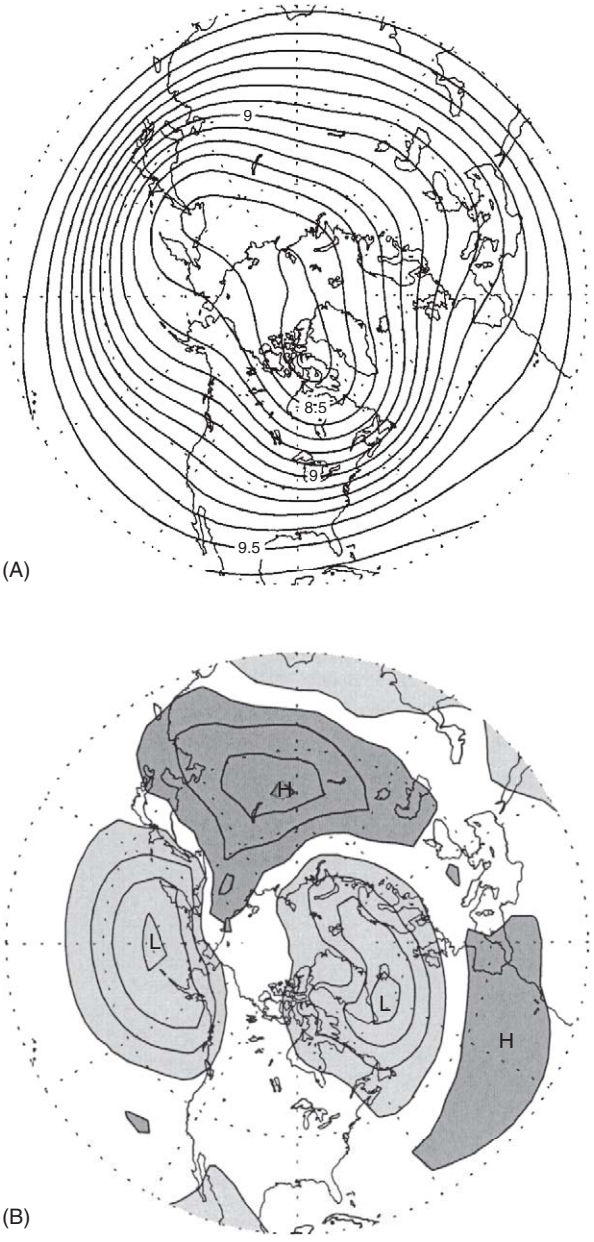

Figure 1 (A) Average height of the 300 hPa pressure surface in northern winter months (December, January, February, and March: DJFM). The average is over 20 winter seasons (December 1979 through March 1999), and is computed from the reanalysis fields produced by the US National Center for Environmental Prediction (NCEP). The contour interval is 100 m. (B) Average sea-level pressure (SLP) for the same months and years, with a contour interval of 5.0 hPa. Sea-level pressure data come from Trenberth's analysis, which is archived at NCAR. Dark (light) shading represents values above 1015 hPa (below 1010 hPa). The letters 'L' and 'H' designate the prominent centers of action: the Aleutian Low, Siberian High, Icelandic Low, and the Azores High. Map domain begins at 20° N.

sea-level pressure field can be broadly characterized as being high over the continents and low over the comparatively warmer northern oceans. Since sea-level pressure is related to column temperature, vertical coherence of the continent–ocean temperature contrast in the lower troposphere is key, as discussed later.

The stationary wave pattern changes considerably between the surface and 300 hPa, and these changes are highlighted in **Figure 2**. The top panels show eddy heights at the 300 and 850 hPa levels, revealing the troughs and ridges. These features are displaced westward with increasing height, i.e., westward tilted, assuming that the same features are being tracked at the two levels. The low-level trough over the Pacific is positioned 15–20° westward of the Aleutian Low, and gives way to a trough centered on the east Asian coast at 300 hPa, which is associated with the Asian–Pacific jet. The 850 hPa trough over the North Atlantic is likewise shifted relative to the Icelandic Low, and migrates further westward towards Hudson Bay at upper levels; it brings cold Arctic air into the central and eastern United States and Canada. The low-level feature over Eurasia (**Figure 2B**) is more definitely linked to the surface Siberian High, but there is no corresponding feature of significance present at the upper level – in contrast with the vertically coherent structure of the Azores High.

The vertical structure of stationary waves is plotted in **Figures 2C** and **D**, which are cross-sections of the eddy height field at 40° N and 60° N. The shading in these panels depicts the eddy temperature field. (In hydrostatic balance, this is the vertical derivative of the height field in $\log(p)$ coordinates.) These plots allow for the tracking of features. The northern section shows the pronounced westward tilt of the east Asian trough, the Rocky Mountain ridge, and the Azores High. The tilt is a consequence of meridional temperature advection by the associated geostrophic wind, which induces cooling to the west (east) of the low (high). Interestingly, connection with the prominent surface features is not strong, except in case of the highs. The Aleutian and Icelandic Lows, in particular, are quite shallow ($p \gtrsim 800$ hPa), exhibiting little connectivity to the westward displaced upper-level troughs. The southern section (40° N) nicely reveals the limited vertical extent of the Siberian High, in contrast with the deep structure of the Azores High.

Comparison of the two cross-sections indicates a striking difference in vertical variation of the eddy heights, particularly in the Eastern Hemisphere. In the northern section, the wave amplitude keeps growing with height up until the tropopause, and even beyond. The structure is indicative of upward propagation of stationary wave energy into the polar lower stratosphere. (Note that the wave's phase is stationary, so the phase velocity is zero, but its group velocity – the

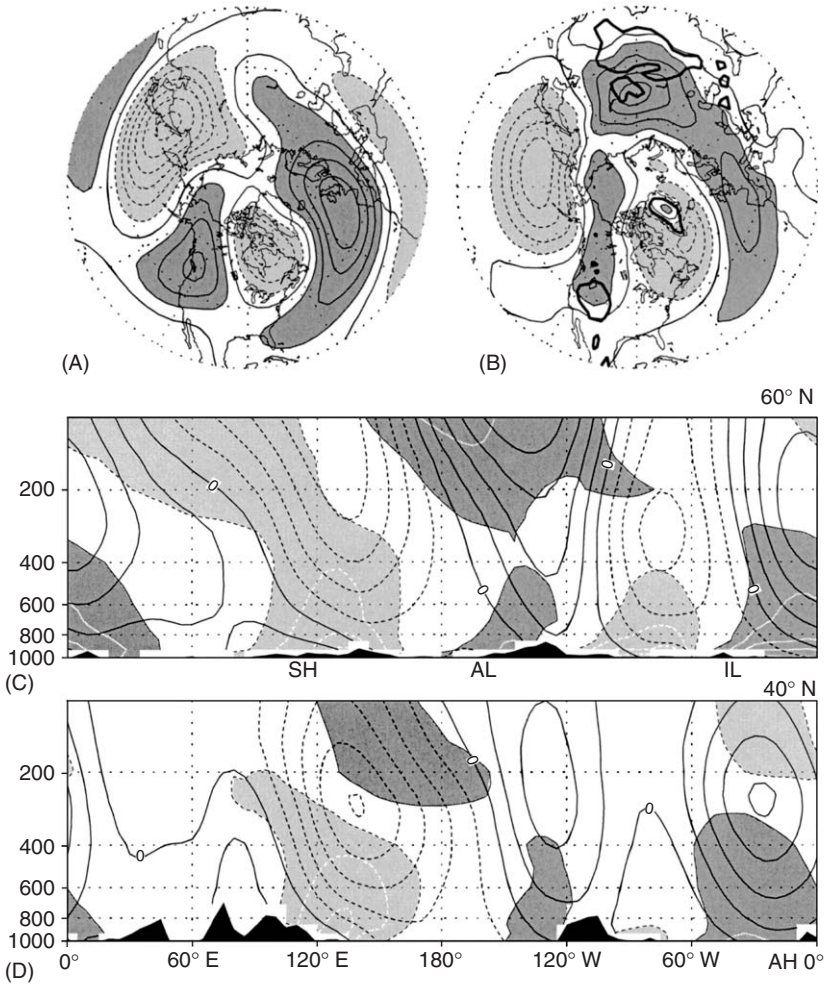

Figure 2 (A) Eddy height at 300 hPa during northern winter (DJFM), or height of the 300 hPa pressure surface after subtracting the zonal average. The contour interval is 50 m, with dark (light) shading for positive (negative) values in excess of 50 m. (B) Eddy height at 850 hPa for the same period, with a contour interval of 25 m and dark (light) shading for positive (negative) values in excess of 25 m. The thick contours in B enclose regions where the surface pressure is less than 850 hPa. In these regions, the pressure surface is interpolated below ground. (C and D) 1000–100 hPa zonal–vertical cross-sections of eddy height and temperature at (C) 60° N and (D) 40° N. Contour interval for eddy height is 50 m, and dashed contours represent negative values. Eddy temperature is plotted in 3 K contours with dark (light) shading for positive (negative) values in excess of 3 K, and zero contours suppressed. 'SH', 'AL', 'IL', and 'AH' are the surface lows and highs of **Figure 1B**.

velocity of energy propagation – is not zero.) In contrast, the 40° N structure is indicative of trapping of wave energy within the troposphere. The eddy height at the 10 hPa level, displayed using shaded contours in **Figure 3**, reveals the presence of a large-amplitude stationary wave at an altitude of nearly 30 km. The zonal wavelength of this pattern is evidently close to the circumference of the latitude circle, i.e., the largest possible. Both observations and theory (*see* **Rossby Waves**) suggest that disturbances of such large wavelengths can propagate into the stratosphere. The wave pattern in **Figure 3** moves the center of the polar vortex away from the geographical pole and reduces the strength of the vortex.

Equatorial westerly duct An important circulation feature in the deep tropics during northern winter is the presence of strong upper-level westerlies ($\sim 10\,\mathrm{m\,s^{-1}}$) over the Pacific and Atlantic longitudes. This is notable because the equatorial belt is otherwise occupied by easterly winds. Zonal winds at 200 hPa are shown in **Figure 4A**, with the easterly region shaded. A vertical section at the equator (**Figure 4B**) shows westerly zones to be confined to the near-tropopause region (100–300 hPa), with maximum values ($\sim 15\,\mathrm{m\,s^{-1}}$) at 200 hPa. The origin of equatorial westerly zones is not well understood, but their absence in northern summers and El Niño winters suggests that their occurrence is linked to the absence of

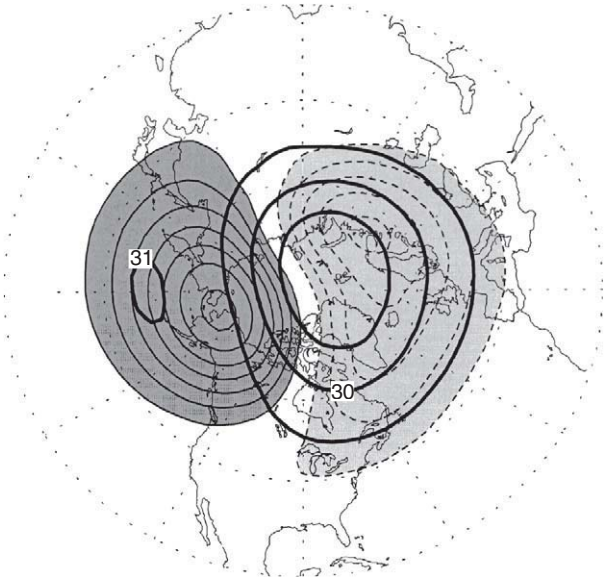

Figure 3 Average height of the 10 hPa pressure surface in northern winter (DJFM). Thick contours show the height field in 500 m increments. The eddy height is plotted at 100 m intervals, with dark (light) shading for positive (negative) values in excess of 100 m. The zero contour for eddy height is suppressed.

strong convection in the central equatorial Pacific and Atlantic longitudes.

Rossby wave propagation theory (*see* **Rossby Waves**) suggests that tropical easterlies are an effective dynamical barrier, shielding the equatorial zone from the influence of midlatitude perturbations. Openings in this barrier, or westerly ducts, thus provide a conduit for equatorward penetration of midlatitude waves during northern winter – a timely opening, since the midlatitude stationary and transient wave activity is most vigorous in winter. Interaction between midlatitudes and the equatorial zone can impact convection and water vapor distribution in the tropics and subtropics. Lateral mixing from extratropical intrusions can also influence tracer transports.

Northern Hemisphere Summer Structure

The northern polar vortex is much weaker in summer than in winter. The summer vortex is shown at the 150 hPa level in **Figure 5A**, and is evidently quite symmetric. It also lacks the tight meridional gradients that characterized the winter vortex. A somewhat higher level was chosen for displaying the summer pattern in order to capture fully the divergent monsoonal flow and accompanying rotational circulations over the warmer landmasses. The upper-level asymmetries include the very prominent anticyclone over Tibet, and troughs over the subtropical ocean basins which are easier to appreciate in the eddy height plots, shown later.

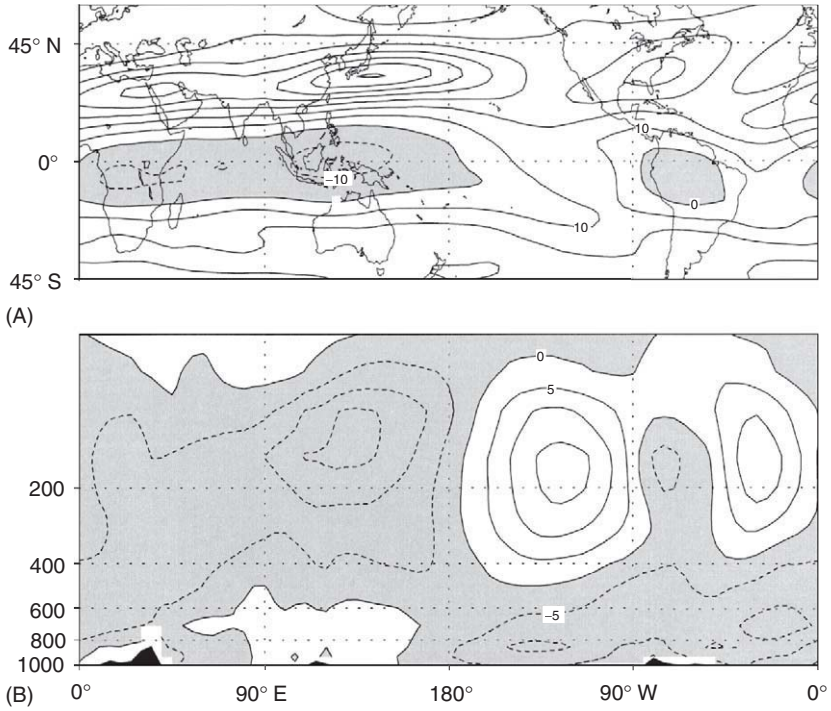

Figure 4 (A) The 200 hPa zonal wind in northern winter (DJFM), contoured in 10 m s^{-1} intervals. Regions where the zonal wind blows from the east are shaded. (B) Zonal–vertical cross-section of zonal wind at the Equator, contoured in 5 m s^{-1} increments, with shading for easterly regions. Top level in (B) is 50 hPA.

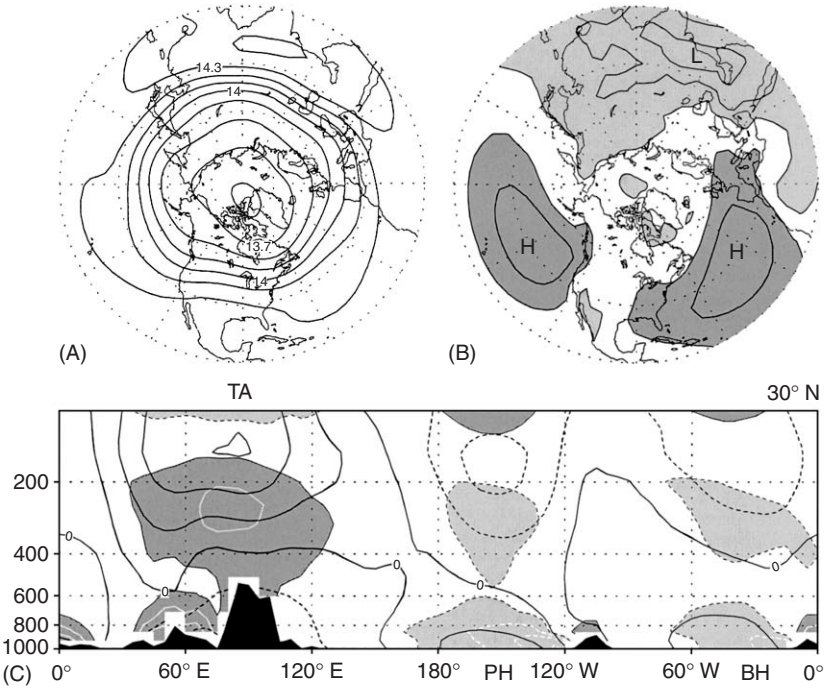

Figure 5 (A) Average height of the 150 hPa pressure surface in northern summer months (June, July, and August: JJA). The average is over 20 summer seasons (June 1980 through August 1999), and is computed from NCEP reanalysis. The contour interval is 100 m. (B) Average sea-level pressure for the same months, plotted as in **Figure 1**. The letters 'L' and 'H' designate the prominent centers of action: the Bermuda High, the Pacific High, and the broad region of low pressure associated with the Asian monsoon. Map domain begins at 15° N. (C) The 1000–100 hPa zonal–vertical cross-section of eddy height and temperature at 30° N, with contours and shading as in **Figure 2D**. 'TA' gives the location of the Tibetan anticyclone, which is enclosed by the 14.3 km contour near the top of panel (A).

The summertime sea-level pressure (**Figure 5B**) has almost a reversed winter structure. Two subtropical anticyclones of comparable strength are present in the ocean basins, underneath the upper-level troughs. They are referred to as the Pacific High and the Bermuda High. The Bermuda High is the summer equivalent of the Azores High, which expands while the Icelandic Low retreats northward during the transition from winter to summer. The Pacific sector undergoes a similar winter to summer transition. The subtropical anticyclones constitute the descending branch of the regional Hadley cells which are driven by deep convection in the tropics. Descending motions induced to the northwest of subtropical monsoonal heating may also contribute to anticyclone development.

Over the continents, sea-level pressure is low during summer. A large region of low sea-level pressure is present over Asia beneath the Tibetan anticyclone (which is actually centered over northern India). The continental-scale anticyclone is an integral element of the Asian monsoon circulation, being the rotational response to deep heating.

The cross-section of eddy height at 30° N (**Figure 5C**) shows the internal baroclinic structure that is typically produced by deep heating in the tropics. The Tibetan anticyclone reaches maximum amplitude at 150 hPa, the level displayed in **Figure 5A**. Over the oceans, the structure is also baroclinic, but the Pacific and Bermuda Highs are evidently shallow features – although not as shallow as their winter counterparts in **Figure 2C**. The strong positive temperature centered over the Tibetan plateau is caused by latent heat release in the monsoon rains. On the other hand, negative temperatures over the Pacific and Bermuda Highs are produced, in part, from the long-wave radiative cooling to space.

The eddy height fields during summer are displayed in **Figure 6**. The Tibetan anticyclone is the prominent feature at upper levels. Baroclinic structure is evident in the Northern Hemisphere, with upper-level troughs positioned over the subtropical highs. Also evident at the upper level is a weak ridge over North America that is associated with the local monsoon system, which includes the Mexican monsoon. The western edge of the Bermuda High produces low-level southerly flow, which brings in significant amounts of moisture from the Gulf of Mexico into the US Great Plains. A notable low-level feature in the Southern Hemisphere is the Mascarene High centered south of Madagascar, which generates strong easterlies along its northern flank (recall that the flow around a

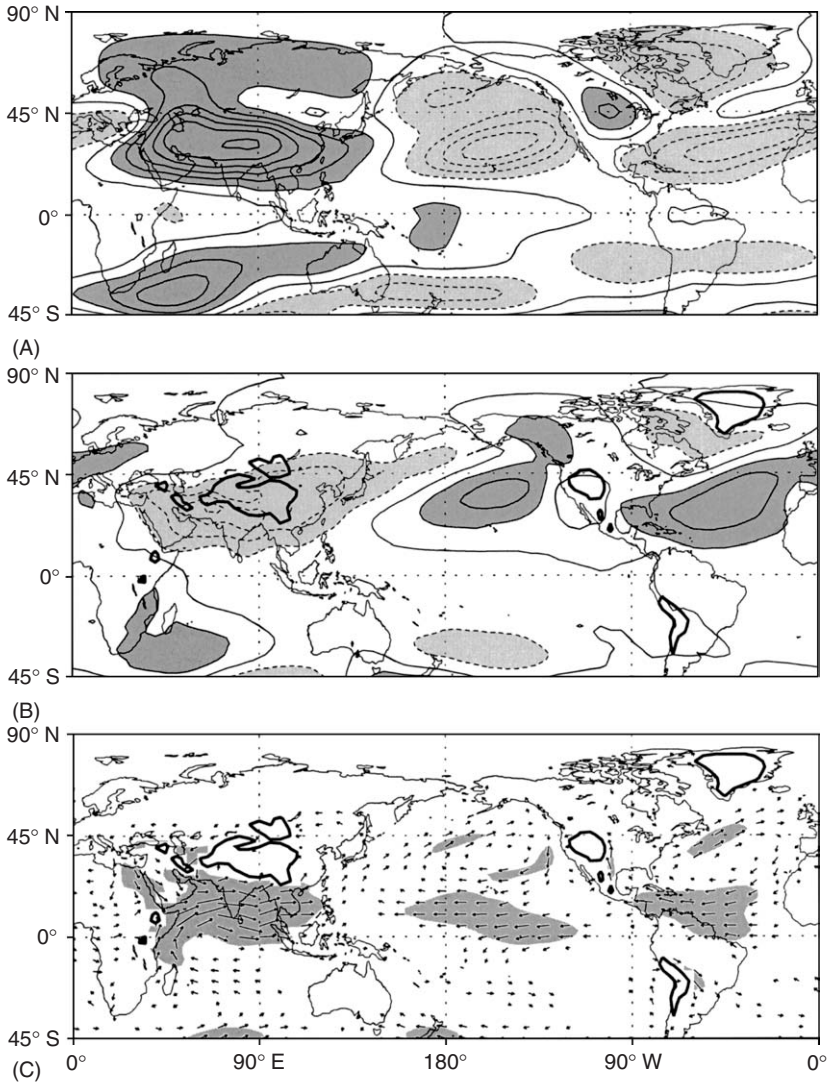

Figure 6 Eddy height at (A) 150 hPa and (B) 850 hPa during northern summer (JJA), with a contour interval of 25 m and dark (light) shading for positive (negative) values in excess of 25 m. (C) Eddy wind vectors at 850 hPa. Regions where the eddy wind speed is in excess of 5 m s^{-1} are shaded, and the longest arrow represents a wind speed of 18 m s^{-1}. Eddy winds with speeds below 2 m s^{-1} are suppressed. As in (B), the thick closed contours in (C) surround mountainous regions where the surface pressure is less than 850 hPa.

Southern Hemisphere High is counterclockwise). After turning northward along the African coast and crossing the Equator, this flow evolves into the southwesterly monsoon flow over the Arabian Sea.

In the Asian monsoon circulation, equatorial and cross-equatorial flows play an important role, and these cannot be appreciated in the height field, since the geostrophic relationship breaks down at the Equator. The summer circulation figures are thus complemented with a vector-wind plot at 850 hPa (**Figure 6C**); only the zonally asymmetric components of winds are plotted. Strong cross-equatorial flow occurs along the east coast of Africa, bringing moisture to the Asian continent. Easterly flow is found all along the Equator, particularly along the southern flank of the Pacific and Bermuda Highs.

Southern Hemisphere Stationary Waves

The Southern Hemisphere has much less land than the Northern Hemisphere, resulting in weaker asymmetries at its lower boundary. A more zonally symmetric circulation, with smaller-amplitude stationary waves, is thus expected. Due to the larger fraction of ocean, the seasonal cycle will also be muted. The seasonal change in surface temperature, for example, will be smaller than in the Northern Hemisphere.

The southern vortex is shown during the December–March (southern summer) and June–August (southern winter) periods in **Figure 7**. As before, the winter vortex is shown at 300 hPa and the summer one at the higher 150 hPa level. Thick lines mark the height

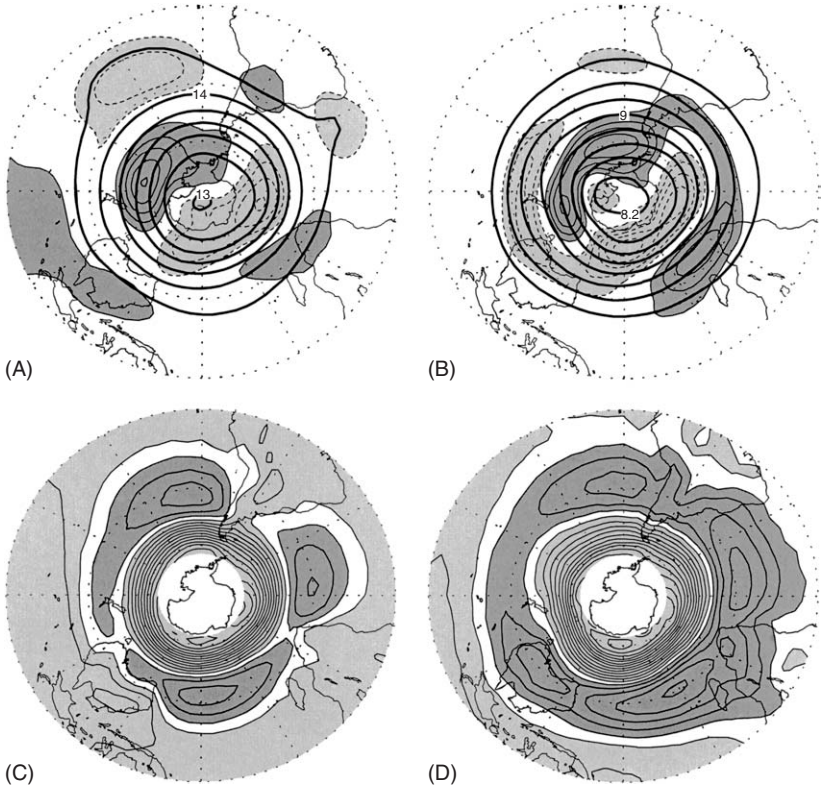

Figure 7 (A) Height of the 150 hPa pressure surface in the Southern Hemisphere during DJFM months (southern summer). (B) Height of the 300 hPa surface during JJA months (southern winter). Thick solid contours show the total height field in 200 m increments, while thin contours represent the eddy height. The contour interval for eddy height is 25 m, with dark (light) shading for positive (negative) values in excess of 25 m. The zero contour for eddy height is suppressed. (C, D) Sea-level pressure for (C) DJFM and (D) JJA months, in 2.5 hPa increments, with dark (light) shading for values above 1015 hPa (below 1012.5 hPa). Map domain is from the Equator to the South Pole. Sea-level pressure values over Antarctica are unreliable and hence suppressed.

contours while the shaded region shows the corresponding eddy height patterns. Note that in the Southern Hemisphere the flow around a low is clockwise rather than counterclockwise. The southern vortex is considerably more symmetric than the northern one. Eddy heights are thus smaller, and contoured at 25 m in both summer and winter (**Figure 7**). The summer and winter patterns are both dominated by the wave number 1 component in the high latitudes so that opposite points along a latitude circle have opposite polarities. The wave component exhibits similar phase and amplitude structure in the two seasons, indicating a significant role of Antarctic orography in its forcing. The subtropics shows greater seasonality, with a ridge over northern Australia in summer; this upper-level feature is linked to the Australian monsoon outflow.

The extent of zonal asymmetries at the surface is examined using sea-level pressure which is contoured with a 2.5 hPa interval as opposed to 5.0 hPa in the Northern Hemisphere. The summer distribution (**Figure 7C**) is much like the one in the Northern Hemisphere (**Figure 5B**), with high-pressure cells occupying the midlatitude ocean basins. In summer, the subtropical highs are interrupted by continental heat lows, caused by the warmer land temperatures. The winter sea-level pressure (**Figure 7D**) is more zonally symmetric, unlike the Northern Hemisphere where asymmetries are most pronounced during winter (cf. **Figures 1** and **2**). A prominent feature of the southern winter pattern is the Mascarene High extending from Africa to Australia, which generates strong south-easterly flow along its northern flank. Its linkage with south-westerly flow over the northern Indian Ocean and Asian summer monsoon can be seen in **Figure 6C**.

The vertical structure of Southern Hemisphere stationary waves is shown in **Figure 8** at 30° S in summer and 60° S in winter – the latitude of the subtropical highs and the polar wavenumber 1 pattern, respectively. Contour intervals in **Figure 8A** are 10 m for height and 1.5 K for temperature, as opposed to 50 m and 3.0 K in northern summer (**Figure 5C**). As in the Northern Hemisphere, the subtropical highs have a baroclinic structure with upper-level troughs superimposed on surface highs. The heat lows over

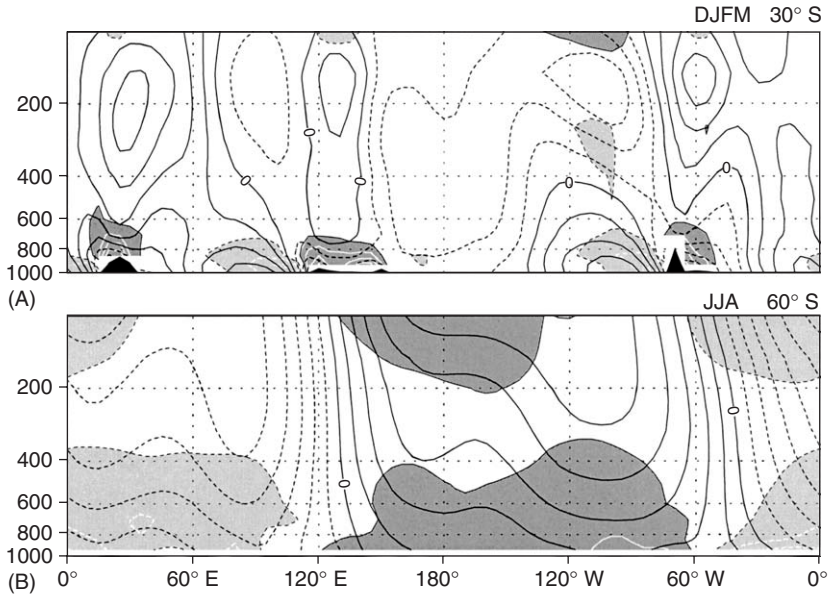

Figure 8 Zonal–vertical cross-sections of eddy height and temperature in the Southern Hemisphere at (A) 30° S in DJFM and (B) 60° S in JJA months. In (A), the contour interval for eddy height is 10 m, with dashed contours for negative values. The contour interval for eddy temperature in (A) is 1.5 K, with dark (light) shading for positive (negative) values in excess of 1.5 K, and zero contours suppressed. In (B), contour intervals for eddy height and temperature are 25 m and 1.5 K, respectively, with plotting conventions as in panel (A).

Australia and southern Africa are quite shallow and intense: this is typical of arid regions where rainfall and mid-tropospheric latent heating do not occur in response to the surface heat low. The winter height and temperature structures (**Figure 8B**) are plotted using 25 m and 1.5 K intervals, as opposed to 50 m and 3.0 K in northern winter (**Figures 2C, D**), due to their relative weakness. The southern winter pattern evidently changes little with height. There is much less westward tilt in comparison with the northern winter structure (**Figure 2C**), indicating less upward propagation of wave energy. Although westerlies are necessary for upward propagation, theoretical considerations suggest that propagation is hindered by the presence of excessive westerlies (westerlies exceeding the Rossby critical velocity), the southern winter vortex is substantially stronger than its northern counterpart (cf. **Figures 1A** and **7B**; note the larger contouring interval in the latter figure).

Transience in the Atmosphere

The above review of stationary wave structure does not convey the extent to which these waves are representative of the instantaneous circulation. For example, how stationary (or transient) is the upper-level circulation during northern winter? Can the stationary waves be 'seen' on synoptic weather charts? The degree to which these charts depart from the climatological pattern is a measure of the strength of the transient flow. Transient activity is estimated in northern winter in **Figure 9** because it is expected to be strongest in this season. The greater vertical shear of the thermally balanced Asian–Pacific and Atlantic jets in winter makes them prone to hydrodynamic instability, which in the context of geostrophic flows is called baroclinic instability. Baroclinic instability produces transient disturbances on subweekly time scales.

The extent to which the stationary wave structure is representative of instantaneous flow is depicted in **Figure 9** by projecting the daily, instantaneous (00UTC), 300 hPa circulation on the climatological wave pattern (**Figure 2A**) during the winters of 1980/81 and 1989/90. Correlation – a measure of the structural similarity of the two maps (without regard to amplitude) – is plotted on the y-axis. The correlation ranges from 0.2 to 0.8 in these winters, indicating that the climatological pattern accounts for up to 65% of the spatial variance. High correlation is however achieved only on a few days in each winter. More typically, the correlation is between 0.5 and 0.6. Interestingly, the correlation drops and recovers over a 2–3 week period, 1–2 times each winter, revealing the establishment time scale of the climatological pattern. Dynamical analysis of such episodes, especially of the recovery phase, can shed light on the establishment mechanisms of stationary waves.

The question of whether the climatological wave pattern can be 'seen' on synoptic charts is addressed in **Figures 9B** and **C**, which show the instantaneous

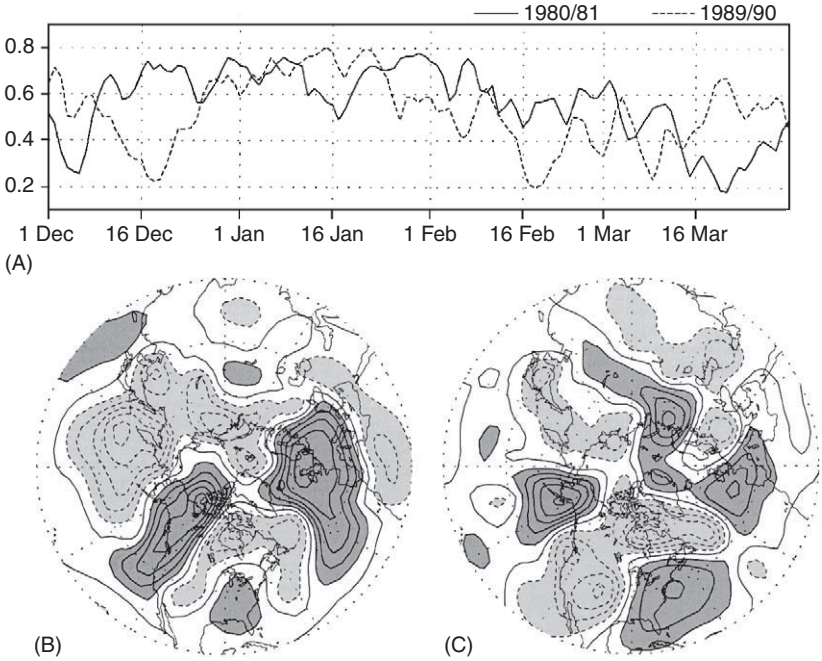

Figure 9 (A) Spatial correlation between the instantaneous (00UTC) and climatological 300 hPa eddy heights during 1980/81 (solid curve) and 1989/90 (dashed curve) winters. Correlations are area weighted and include height data from 20° N to the north pole. (B) 300 hPa eddy height on 1 February 1981, when the spatial correlation was 0.74. (C) Eddy height on 16 February 1990, when the correlation was 0.29. In (B) and (C), the contour interval is 100 m (twice the interval in **Figure 2A**), with dark (light) shading for positive (negative) values in excess of 100 m.

(00UTC) wave pattern on two days: 1 February 1981, when the spatial correlation is high (0.74; **Figure 9B**), and 16 February 1990, when the correlation is low (0.29; **Figure 9C**). The climatological pattern (**Figure 2A**) can be clearly recognized in the former plot, but not in the latter. Even when structurally similar, the patterns can evidently have very different wave amplitudes; the contour interval is 50 m in **Figure 2A** but 100 m in **Figure 9B**.

Forcing of Stationary Waves

Stationary waves are generated, ultimately, by the zonal asymmetries at the Earth's surface: orography, continent–ocean contrasts, and sea surface temperature gradients. Through dynamic and thermodynamic interactions with the zonal-mean flow, and subsequent mutual interactions, surface inhomogeneities produce zonally asymmetric circulation and precipitation features at upper levels. Comprehensive numerical models of the atmosphere, which include coupling between physical and dynamical processes, are able to realistically model the observed stationary waves. In a sense, the often posed question – on relative contribution of orography and other processes in forcing of stationary waves – has been addressed by such prognostic general circulation models (GCMs). Comparison of GCM simulations obtained with and without orography provide insight. In these assessments, the change in the heating distribution is attributed to orographic forcing, whose circulation impact is found to be comparable to that of all other processes put together.

Historically, answers to the above question were sought in a framework where 'orographic forcing' was used more restrictively – to refer to the dynamical forcing of flow from mechanical diversion. In such analysis, the entire heating distribution, regardless of its origin (e.g., from condensation in adiabatically cooled upslope flow), was regarded as an independent forcing. This framework was adopted, perhaps, because mechanical diversion of flow by an orographic barrier is conceptually easier to model. Such studies lead to the rapid advancement of stationary wave theory, including construction of potential vorticity conserving models for the responses to orography, meridional and vertical wave propagation analysis, and understanding of troposphere–stratosphere interaction.

Theoretical Considerations

Large-scale atmospheric motions in the extratropics are approximately hydrostatic and quasi-geostrophic (QG) in character. The hydrostatic approximation recognizes the operative balance between the

horizontally varying pressure and density perturbations, while the QG approximation acknowledges the near-balance between the Coriolis force and the horizontal pressure gradient. QG flow is thus dominated by the rotational component. Its evolution, however, is determined, in part, by the comparatively weaker divergent flow component, as described by the vorticity equation

$$\frac{\partial \zeta}{\partial t} + \mathbf{V}_\mathrm{h} \cdot \boldsymbol{\nabla}\zeta + \beta v = -(f+\zeta)(\boldsymbol{\nabla} \cdot \mathbf{V}_\mathrm{h}) \qquad [1]$$

Here, ζ is the QG relative vorticity $(= \hat{\boldsymbol{k}} \cdot (\boldsymbol{\nabla} \times \mathbf{V}_\mathrm{h}) = \boldsymbol{\nabla}^2 \psi)$, ψ is the geostrophic streamfunction, f is the Coriolis parameter with $\partial f/\partial y = \beta$, and $\mathbf{V}_\mathrm{h}$ is the horizontal QG flow. The right-hand term is the product of absolute vorticity $(f+\zeta)$ and horizontal convergence, and is often called the 'stretching term' because convergent flow leads to stretching of vortex tubes.

Due to compressibility of air, evolution of the thermodynamic state is conveniently described using potential temperature, $\theta = T(p_0/p)^{R/C_\mathrm{p}}$, which is conserved in adiabatic motion; p_0 is the reference pressure (1000 hPa). Potential temperature thus changes only in response to diabatic heating $\dot{Q}$, as follows:

$$\frac{\partial \theta}{\partial t} + \mathbf{V}_\mathrm{h} \cdot \boldsymbol{\nabla}\theta + w\frac{\partial \theta}{\partial z} = \frac{\dot{Q}}{C_\mathrm{p}}(\theta_0/T_0) \qquad [2]$$

where $\theta_0 = T_0(p_0/p)^{R/C_\mathrm{p}}$, with $T_0 = T(p_0)$.

Since stationary waves refer to the zonally varying component of the flow (here onward denoted by prime), their dynamics can be described, to first order, by linearizing eqns [1] and [2] about the zonal-mean circulation, $\bar{U}(y, z)$ and $\bar{\theta}(y, z)$. The linearized equations are valid for small-amplitude perturbations:

$$\zeta'_t + \bar{U}\zeta'_x + v'(\beta - \bar{U}_{yy}) \approx -f(\boldsymbol{\nabla} \cdot \mathbf{V}'_h) \qquad [3]$$

$$\theta'_t + \bar{U}\theta'_x + v'\bar{\theta}_y + w'\bar{\theta}_z \approx (\dot{Q}'\theta_0/T_0 c_p) \qquad [4]$$

For convenience, subscripts are used to denote the partial derivatives.

Orographic Forcing and Response

The forcing and propagation of stationary waves can be discussed using eqns [3] and [4]. In contrast with diabatic heating, which is explicitly present as right-hand forcing in the thermodynamic equation, the mechanical forcing by orography (h') is implicitly present through its kinematic impact on vertical velocity at the lower boundary (w_s). In the presence of the zonal-mean circulation, the linearized vertical velocity, w'_s, equals $\bar{U}h'_x$.

In simplified treatments of orographic interaction, the geophysical fluid is additionally considered to be homogeneous and incompressible $(\boldsymbol{\nabla} \cdot \mathbf{V}_\mathrm{h} = -\partial w/\partial z)$, so that response is determinable using the vorticity equation alone – this 'shallow water' approximation is indeed reasonable for the interaction of oceanic flows with underwater topography, but somewhat limited in capturing aspects of the atmospheric interaction. In shallow water theory, density (or temperature) is constant, and the horizontal flow, including horizontal divergence, is height independent. Assuming that a rigid lid is placed at the top of the fluid $(z = H)$, so that vertical velocity vanishes there, one obtains $\partial w'/\partial z \approx -(\bar{U}h'_x)/H$. The forced waves are then modeled by eqn [5], where $\bar{U}$ has been additionally assumed to be latitude independent, and perturbation vorticity is dissipated (e.g., by Ekman spin-down) on an ε^{-1} time scale:

$$[\partial/\partial t + \bar{U}\,\partial/\partial x + \varepsilon](\psi'_{xx} + \psi'_{yy}) + \beta\psi'_x \approx -(f/H)\bar{U}h'_x \qquad [5]$$

To understand the forced response, consider an arbitrary Fourier component of the geostrophic streamfunction: $\psi'(x, y, t) = \mathrm{Real}\{\hat{\psi}_{k,l} e^{i(kx+ly-\omega r)}\}$, where the hat denotes the complex amplitude corresponding to zonal and meridional wavenumbers, k and l, and associated frequency ω. For such a perturbation, eqn [5] yields the solution

$$\hat{\psi} = \frac{f\hat{h}}{H[(k^2+l^2)(\bar{U}-c)/\bar{U} - \beta/\bar{U} - i\varepsilon(k^2+l^2)/(\bar{U}k)]} \qquad [6]$$

For stationary waves $(\omega = 0)$, the zonal phase speed, $c(= \omega/k)$, vanishes. This simplifies the first term in the denominator to $(k^2 + l^2)$. In the presence of dissipation, the orography and streamfunction are not in phase, since the denominator in eqn [6] is complex. The possibility of resonance is also indicated in the inviscid case $(\varepsilon = 0)$, when $(k^2 + l^2) = \beta/\bar{U}$. Dissipation however limits the wave amplitude at resonance, with $\hat{\psi} \propto i\hat{h}$. The streamfunction and orography are 90° phase-shifted (or in quadrature) in this case, with the trough in the flow being a quarter wavelength downstream of the mountain ridge. When forcing is on larger scales, $(k^2 + l^2) < \beta/\bar{U}$, planetary vorticity advection dominates zonal advection of relative vorticity in balancing the orographically induced vorticity on upslopes and downslopes. Both the real and imaginary parts of the denominator in eqn [6] are negative in this case, which puts the trough within a quarter wavelength downstream of the ridge.

It is interesting that troughs in the observed 300 hPa stationary wave pattern (cf. **Figure 2A**) are also downstream of the orographic features, but the extent to which these are forced by local orography remains somewhat uncertain, as discussed later. Also, the assumed Fourier representation of the streamfunction implies the presence of meridional boundaries which confine wave energy to a midlatitude channel – a set-up conducive for resonance. The sinusoidal zonal structure is also unrealistic, since orographic features are generally localized. In nature, the wave energy propagates away zonally, meridionally, and vertically from the localized forcing region, thus calling into question the validity of the solution [6].

The pedagogically useful shallow-water model of orographic interaction is limited for other reasons as well. The tropospheric flow cannot be assumed to be homogeneous and incompressible, since cooling (heating) from adiabatic expansion (compression) during ascent (descent) is important in the thermodynamic budget. Moreover, a flow configuration which satisfies the vorticity eqn [3] can be unbalanced from the viewpoint of this budget. For example, when planetary vorticity advection dominates the left-hand side in balancing the upslope divergent flow in eqn [3], the thermodynamic budget [4] is unbalanced in the absence of condensation heating (precipitation), since both adiabatic ascent and equatorward flow lead to colder temperatures. The generation of orographic response must thus be understood by considering the vorticity and thermodynamic equations together, so that any implications that one may have for the other are fully accounted for. Such considerations lead to the development of the QG potential vorticity equation.

QG Potential Vorticity Equation

The prediction equation for QG flow that does not explicitly reference the divergent flow component is called the QG potential vorticity equation. Although it can be derived quite generally, the focus here is on its simplified linearized version, when the zonal-mean flow $\bar{U}$ is independent of latitude. The equation is derived by eliminating the divergent flow from eqns [3] and [4]. In the $z^* = (RT_0/g)\ln(p_0/p)$ coordinate, which reduces to geometric height in an isothermal atmosphere, the QG potential vorticity equation is

$$q'_t + \bar{U}q'_x + v'\bar{q}_y = \frac{R}{Hc_p\rho_0}\frac{\partial}{\partial z^*}\left(\frac{\rho_0\dot{Q}'}{N^2}\right) \qquad [7]$$

where

$$q'(x, y, z) = \psi'_{xx} + \psi'_{yy} + \frac{f^2}{N^2\rho_0}\frac{\partial}{\partial z^*}\left(\rho_0\frac{\partial\psi'}{\partial z^*}\right)$$

and

$$\bar{q}_y(z) = \beta - \frac{f^2}{N^2\rho_0}\frac{\partial}{\partial z^*}\left(\rho_0\frac{\partial\bar{U}}{\partial z^*}\right) \qquad [8]$$

Since divergent flow is not referenced by this equation, it is of some interest to examine the manifestation of orographic forcing in this analysis framework. Not surprisingly, this forcing enters as a lower boundary condition, but in the thermodynamic equation [4]. This is because of the direct reference to vertical velocity in eqn [4], in contrast with the vorticity equation [3] which refers only to its vertical gradient. With $w'_s = \bar{U}h'_x$, the boundary condition conveying orographic forcing is

$$\theta'_t + \bar{U}\theta'_x + v'\bar{\theta}_y = -\bar{U}h'_x\bar{\theta}_z + (\dot{Q}'\theta_0/T_0c_p) \text{ at the surface} \qquad [9]$$

Assume for purposes of this discussion that diabatic heating vanishes at the surface, so that only adiabatic cooling (warming) is occurring on the upslope (downslope). In steady flows, the heating can be balanced by zonal eddy advection and/or meridional advection of mean temperature. If upslope cooling is compensated by the latter, the upslope flow will be poleward, and a high-pressure center will be positioned over the mountain ridge near the surface. The response at upper levels depends upon the zonal scale of mountains: large wavelengths will propagate into the lower stratosphere, and phase lines will tilt westward with increasing height, all as depicted in the **Figure 10A** schematic. It is interesting that although thermal advection and vertical wave propagation are absent in the shallow water model, the horizontal structure of the long-wavelength solution (in the presence of damping, eqn [6]) is not too different from that indicated at upper levels in **Figure 10A**.

Heating Response

The stationary wave response to heating can be qualitatively understood from the thermodynamic equation [4]. In the deep tropics, horizontal variations of geopotential (and temperature) are much smaller since it is difficult to maintain them in the presence of the weak Coriolis force. Consequently, horizontal temperature advection is ineffective in balancing diabatic heating in eqn [4]. Away from the surface, heating is thus balanced, almost entirely, by adiabatic cooling, with the vertical

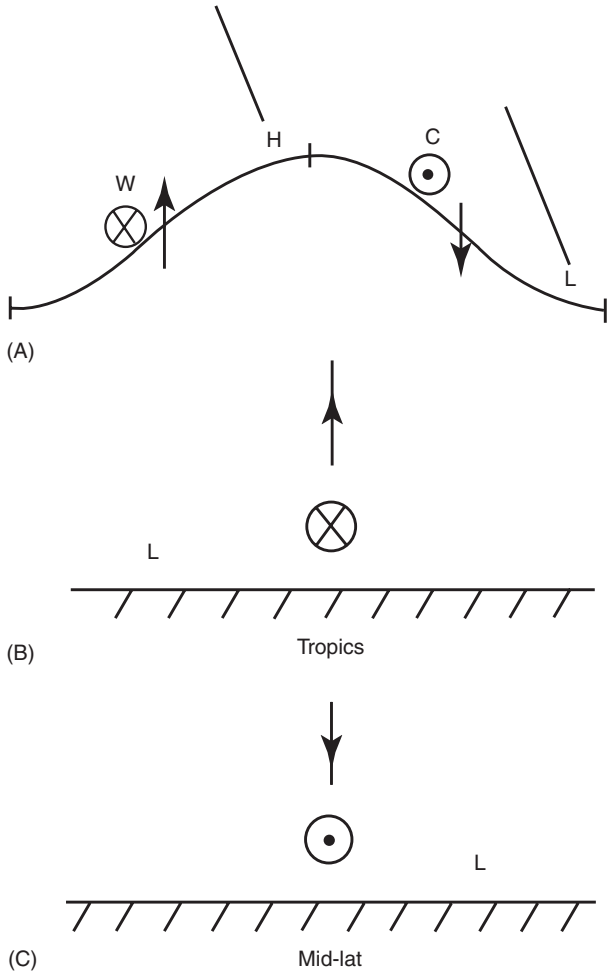

Figure 10 Schematic depiction of the longitude–height response forced by (A) westerly flow over midlatitude orography, (B) tropical heating, and (C) midlatitude heating, all taken from Hoskins and Karoly (1981). The orographic response is shown for the long-wavelength case, and is determined from both dynamic and thermodynamic (i.e., quasi-geostrophic potential vorticity) considerations. The arrows depict vertical motion, and circled crosses and dots denote poleward and equatorward flow, respectively. H and L denote the pressure ridge and trough, with the lines showing the vertical tilt of the pressure wave. W and C are the warmest and coldest air, respectively.

profile of w' closely following that of heating. A substantial portion of heating in the tropics results from deep convection, which produces strongest heating in the mid-to-upper troposphere, as shown later in **Figure 11C**. Such heating distribution leads to convergence (divergence) in the lower (upper) troposphere, which results in vortex stretching (squashing). The rotational response to the induced vorticity depends on the horizontal forcing scale: if the scale is large, the stretching is offset by poleward advection of planetary vorticity, which is tantamount to the surface low being positioned westward of the heat source, as schematically illustrated in **Figure 10B**.

In the midlatitudes, heating does not extend as deeply into the troposphere as in the tropics. Heating in the Pacific and Atlantic stormtracks, for example, is confined mostly to the lower troposphere, as shown later in **Figure 11B**. Midlatitude heating is offset to a large extent by horizontal temperature advection; larger temperature gradients are sustainable in midlatitudes due to the greater Coriolis force. Large-scale heating in midlatitudes is balanced, mostly, by cold advection from the north; the near-surface low is thus positioned eastward of the heating. Interestingly, vertical motion in the vicinity of midlatitude heating is determined by vorticity balance considerations – a complete reversal of the tropical situation: cold advection from the north brings with it higher vorticity air as well, and this induced vorticity advection must be offset if a steady state is to be maintained. The compensation is accomplished by vortex compression, which has implications for the temperature field.

Wave Propagation

The qualitative arguments discussed above are helpful in understanding the nature of response in the forcing region. The stationary wave response is however not confined to the forcing region alone, since Rossby waves propagate zonally, meridionally, and vertically, carrying the disturbance (energy) into the far field (unforced region). The energy propagation, or group velocity, characteristics depend both on the perturbation scale and structure of the basic state. Some zonal-mean zonal wind configurations encourage Rossby wave propagation, while others impede it. Basic state flow can thus profoundly impact wave propagation into the tropics and the stratosphere.

Theoretical analysis helps to focus on the basic state attributes that are influential, e.g., the direction and curvature of the zonal-mean zonal wind. A useful quantity in wave propagation analysis is the refractive index which seizes on these and other relevant attributes. A display of refractive index variations is often helpful, since it conveys, to first order, the wave propagation pathways, as waves are generally refracted towards higher refractive index regions. Such analysis suggests that midlatitude stationary waves are refracted towards the Equator, drawn there by the large index values resulting from diminishing westerly winds. The tropical easterlies, in contrast, present an effective dynamical barrier to equatorward propagation of midlatitude stationary waves. In the vertical, waves with large horizontal scales alone can propagate upward, but only when the upper-level westerlies are not too strong.

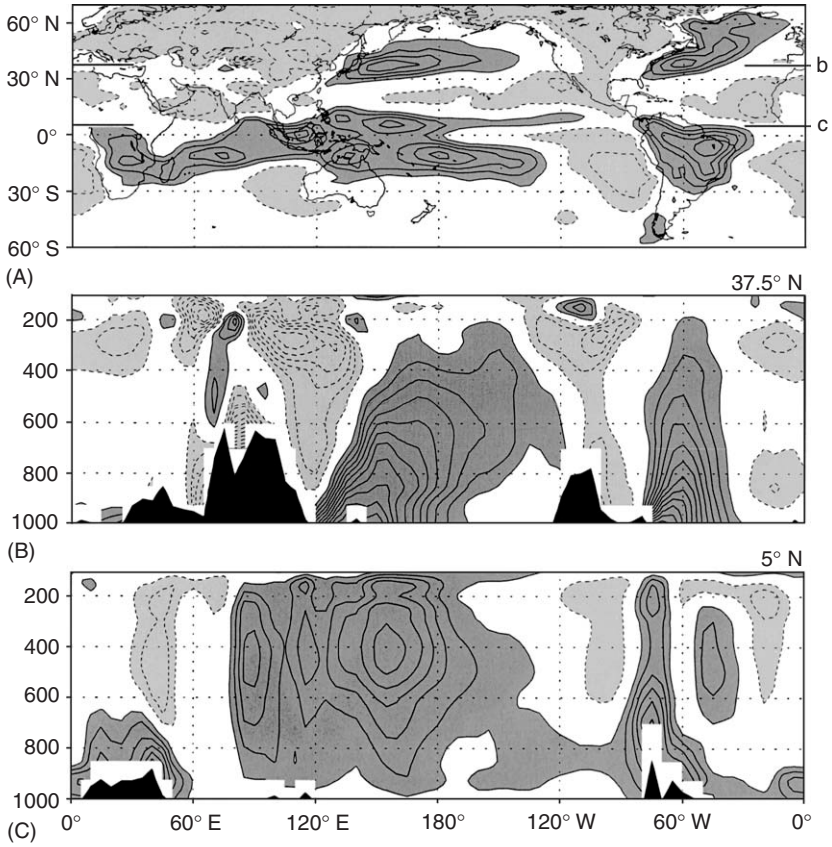

Figure 11 (A) Mass-weighted vertical average of diabatic heating, calculated as a residual from the thermodynamic equation. The winter season (DJFM) diagnosis is obtained from NCEP reanalysis fields for 20 winter seasons (1979/80–1998/99). The contour interval is 0.5 K day^{-1}, with dark (light) shading for positive (negative) values in excess of 0.5 K day^{-1}, and zero contours suppressed. (B, C) Zonal–vertical (1000–100 hPa) cross-section of diabatic heating at (B) 37.5° N and (C) 5° N, with contours and shading as in panel (A). The latitudes of the cross-sections in (B) and (C) are marked with thick lines at the edges of panel (A). A 9-point smoother is applied to the heating field before plotting.

Diabatic Heating in Northern Winter

Diabatic heating plays a prominent role in the forcing of stationary waves. In stationary wave theory, it is an explicit forcing in the QG potential vorticity equation [7], and even orographic forcing in this theoretical framework manifests as surface heating [9].

In nature, heating resulting from the change of phase of water substance, turbulent eddy diffusion, and short-wave and long-wave radiative fluxes is referred to as diabatic heating. (Note that the temperature of air parcels can change even without any diabatic heating, from adiabatic compression or expansion.) In contrast with Earth's orography, whose highly accurate measurements are widely known, the three-dimensional structure of diabatic heating is only beginning to be described. The main reason why the heating distribution has remained uncertain is that, unlike other quantities, heating is not directly measured. It is, instead, estimated, usually as a residual in the thermodynamic budget. Since the heating estimate is only as good as the quality of atmospheric data from which it is diagnosed, the quality of atmospheric analysis is critical for the diagnosis. Fortunately, data coverage and quality and analysis methods have all improved in the last two decades, and are reflected in the modern reanalysis data sets. Heating diagnosis from one such data set, the US National Centers for Environmental Prediction (NCEP) reanalysis, is shown in **Figure 11**.

The mass-weighted vertical average of diabatic heating,

$$\frac{1}{(p_s - 100)} \int_{100}^{p_s} \dot{Q} c_p^{-1} \, dp$$

is shown during northern winter in units of K day^{-1}; here, p_s is the surface pressure, c_p is the specific heat of air at constant pressure, and the integration is from the surface to 100 hPa. Key features in **Figure 10A** include the heating centers in the extratropical Pacific and Atlantic basins, which effectively define the two

midlatitude stormtracks. The northern continents, in contrast, constitute the cooling regions. In the tropics, heating is strong over the South Pacific convergence zone and the Amazon basin. A narrow zone of heating is also present in the Pacific just northward of the Equator; this intertropical convergence zone (ITCZ) is much stronger during northern summer when it is positioned a few degrees farther northward and fully extended across the Pacific basin.

Diabatic heating has a complicated vertical structure which changes with latitude and season. The changes with latitude are shown in **Figures 10B** and **C**, which depict height–longitude cross-sections through the midlatitude stormtracks (37.5° N) and the ITCZ (5° N). The stormtrack heating is evidently strongest near the surface, with peak values close to 6 K day^{-1}, and diminishes rapidly with height. Latent heating due to precipitation in baroclinically unstable synoptic-scale disturbances is the primary contributor to stormtrack heating. Diabatic cooling, on the other hand, is comparatively weaker, and focused more near the tropopause in this estimation, for reasons that are not clear.

The vertical structure of ITCZ heating is strikingly different. Although the entire column is being heated, heating is generally strongest in the mid-to-upper troposphere. For example, over the tropical Pacific warm pool – the site of persistent deep convection – heating is strongest ($\sim$3 K day^{-1}) at 400 hPa. In contrast, heating over land (e.g., equatorial Africa) is strongest near the surface due to sensible heating. The heating structure over Central America is also similar, except that elevated surface heating there has produced some deep convection as well.

Interaction with Transients

The climatological stationary waves coexist with vigorous atmospheric motions occurring on a variety of time scales (**Figure 9**), and there are strong interactions between these transient motions and the stationary waves. Transient motions are the instantaneous departures of the flow from its climatological state, and the time mean of transient motion thus vanishes, by definition. However, fluxes of heat and vorticity by transients do not vanish in general. For example, the contribution of transients to the advection terms in eqn [2] can be written as

$$\begin{aligned}&\mathbf{V}_b'' \cdot \boldsymbol{\nabla}\theta'' + w''\,\partial\theta''/\partial z \\ &\approx \boldsymbol{\nabla}\cdot(\mathbf{V}_b''\theta'') + \partial(\omega''\theta'')/\partial p \qquad [10]\end{aligned}$$

where the double prime denotes the transient component and ω is the vertical velocity in p-coordinates. The right-hand side of eqn [10] is the heat-flux divergence from transient motions. In synoptic systems, northward (southward) transient motions are typically accompanied by positive (negative) temperature fluctuations, so that heat flux diverges to the south of a stormtrack and converges to the north. The heat-flux divergence acts as heat sources and sinks for the time-mean flow, and the stationary waves respond to this thermal forcing just as they respond to diabatic heating. Likewise, the convergence of transient vorticity flux $(-\boldsymbol{\nabla}\cdot(\mathbf{V}_h''\zeta'') - \partial(\omega''\zeta'')/\partial p)$ provides sources and sinks of vorticity for the stationary waves.

The net effect of transient thermal and vorticity fluxes on stationary waves is not easy to characterize. However, it is clear that transient forcing is strong enough in northern winter to exert a powerful influence on stationary waves. The 700 hPa heat-flux convergence by perturbations lasting less than 1 month is superimposed in **Figure 12A** on the local winter eddy temperature pattern. The two fields evidently oppose each other. For example, transient heat fluxes diverge from the warmer regions over the Atlantic and the west coast of North America and converge in the colder regions above north-eastern Canada. Thus, throughout most of the northern midlatitudes, transient thermal fluxes have a damping effect on the lower tropospheric stationary eddy temperature pattern. Furthermore, the forcing by transient thermal fluxes is on the order of 0.5 K day^{-1}, , while the eddy temperatures are about 4 K. In the absence of other processes, it would take little more than a week for the thermal fluxes to reduce dramatically the 700 hPa eddy temperature field. Such a reduction also implies a substantial weakening of the upper-level geopotential pattern, since temperature is the vertical derivative of geopotential in hydrostatic balance.

While transients are an important influence on stationary waves, the stationary waves can be equally influential for the transients. One way in which stationary waves organize transients is by creating localized regions of strong cyclogenesis. Synoptic systems tend to develop in regions of strong lower tropospheric temperature gradients, and such regions are present off the coasts of Asia and North America in **Figure 12A**. The ability of the local temperature gradient to enhance the growth of synoptic systems can be measured by the Eady growth parameter (ε):

$$\varepsilon = 0.31\,\frac{|\boldsymbol{\nabla}T|}{|T(T_0\,\partial\,\ln\,\theta/g\,\partial z)|^{1/2}}$$

Its plot in **Figure 12B** shows large values in the same regions where stormtrack heating occurs in **Figure 11A**. Comparison of these panels suggests that

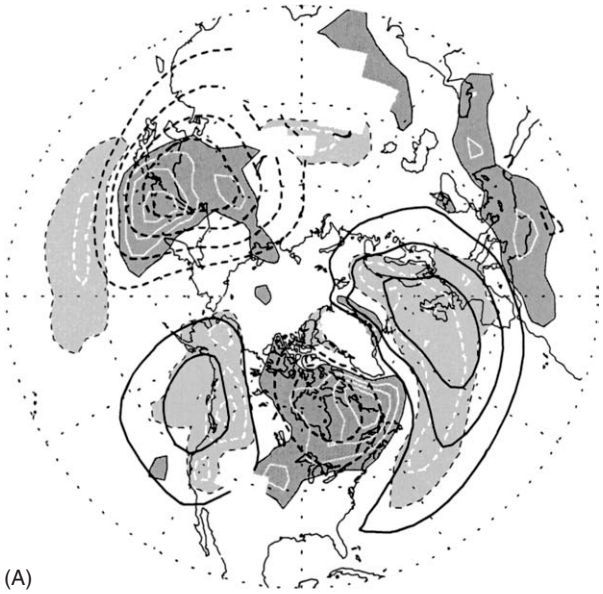

(A)

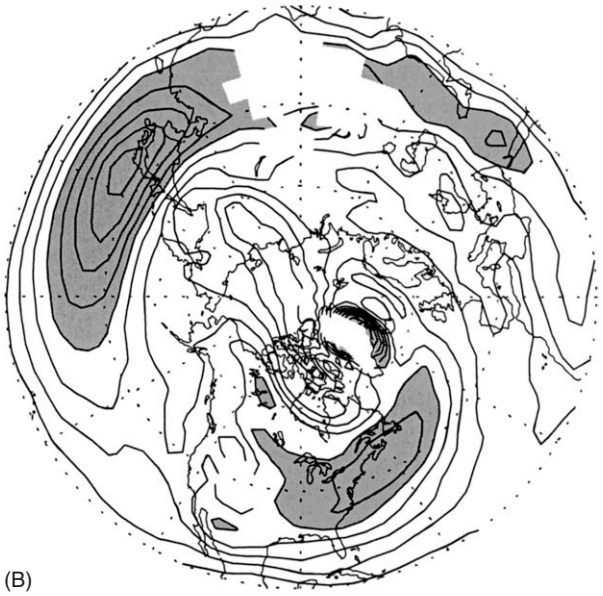

(B)

Figure 12 (A) The 700 hPa eddy temperature (thick contours) and heat-flux convergence by transient motions (shading and white contours) in northern winter months (DJFM). The contour interval for temperature is 2 K, and dashed lines represent negative values. The contour interval for heat-flux convergence is 0.5 K day^{-1}, with dark (light) shading for positive (negative) values in excess of 0.5 K day^{-1}. Zero contours for temperature and heat-flux convergence are suppressed, and regions where the surface pressure is less than 700 hPa are masked out. (B) Eady growth parameter in northern winter (DJFM), calculated from the 700 hPa temperature gradients. The contour interval is 0.1 day^{-1}, with dark shading for values in excess of 0.6 day^{-1}.

stationary waves play an important role in determining the locations of stormtracks. In addition to this effect on growth rate, stationary waves can also have a mechanical effect on stormtracks, by changing the steering winds that determine storm paths and by exchanging mechanical energy with the storms.

The Eady growth rate is applicable to synoptic transients, which grow by extracting energy from the thermal gradients (or vertical shear) of the climatological state. Synoptic systems, in fact, account for less than half of the transient forcing in the vorticity and thermodynamic equations for the climatological stationary waves. Furthermore, the slower transients (those with time scales between, say, 10 days and 1 month) are quite distinct from synoptic transients. They do not generally travel along concentrated stormtracks, nor do they typically grow by extracting energy from the climatological temperature gradients. Although these transients are certainly influenced by the climatological stationary waves, the nature of this influence is rather complex and cannot be easily summarized.

Modeling of Northern Winter Stationary Waves

Modeling of orographically forced stationary waves dates back to the seminal paper of Charney and Eliassen in 1949, in which linear shallow water theory was applied to the longitudinal distribution of orography at 45° N. The earlier discussion here, including the development of eqn [5] and its solution [6], largely follows the analysis reported in that paper. Charney and Eliassen found the midlatitude mountains to be rather influential, accounting for almost all of the observed signal in their analysis.

Since that time, diabatic heating due to continent–ocean contrasts, and transient fluxes of heat and momentum have also been advocated as important mechanisms for the generation of stationary waves. In the intervening period, the atmosphere has been more closely observed, both spatially and temporally, and there has been a tremendous increase in computational power for modeling studies. A reassessment of the relative roles of various forcing mechanisms is thus in order. In effect, more complete versions of the dynamical and thermodynamical equations can now be solved globally at high resolution, and verified against the extensive record of upper-air observations that have been compiled since.

It is still advantageous of linearize the system of equations, at least initially, since this allows the influence of individual forcing terms to be examined separately. Of course, the forcing terms can have strong mutual interactions. For example, heating can cause eddy flow which then impinges on mountains, and the subsequent orographically induced uplift can generate convection and lead to further heating.

However, linear diagnostic models serve a valuable purpose in assessing the relative importance of the different forcing terms in different regions. They also indicate the degree to which linear perturbation theory applies to stationary waves.

A linear simulation of northern winter stationary waves is presented in **Figure 13**. The linear model uses $\sigma = p/p_s$ as the vertical coordinate (here p_s is the surface pressure) so that mountains do not intersect the model levels. There are 15 levels in the vertical, ranging from 1000 to 25 hPa, and the horizontal resolution is 7.5° in the zonal direction and about 2.5° in the meridional direction. As in eqns [3] and [4], the model is linearized about the zonal-mean climatological state. The momentum and thermal dissipation in the model is roughly equivalent to a 5-day damping time scale in eqns [3] and [4]. The forcing consists of three-dimensional diabatic heating (**Figure 11**), orographic height, and transient fluxes of heat and momentum.

The 300 hPa response obtained with all forcings is shown in **Figure 13A**, and plotted using the convention used in **Figure 2A**, with which it should be compared. The linear model can simulate the ridge over the Atlantic, the low off the east Asian coast, and the trough over Canada. A notable flaw in the simulation is the weakness of the ridge over the Rockies. The solution shows that linear perturbation theory can explain many, though not all, aspects of the observed stationary wave pattern.

The model response when forced separately by diabatic heating, mountains, and transients is shown in panels (B)–(D), respectively; note that contour interval in these three panels is half that in panel (A). All three forcings contribute significantly to the total pattern. The heating response includes jets in the Asian–Pacific and Atlantic sectors. Heating is evidently important in establishing the ridge over the Atlantic and northern Europe, and contributes significantly to the trough over Canada as well.

The response to mountains in panel (C) shows troughs downstream of the Himalayan–Tibetan complex and the Rockies, as suggested by the shallow water solution [6] and also QG potential vorticity considerations (cf. **Figure 10A**), in each case for long wavelengths. Thus, orography contributes to the

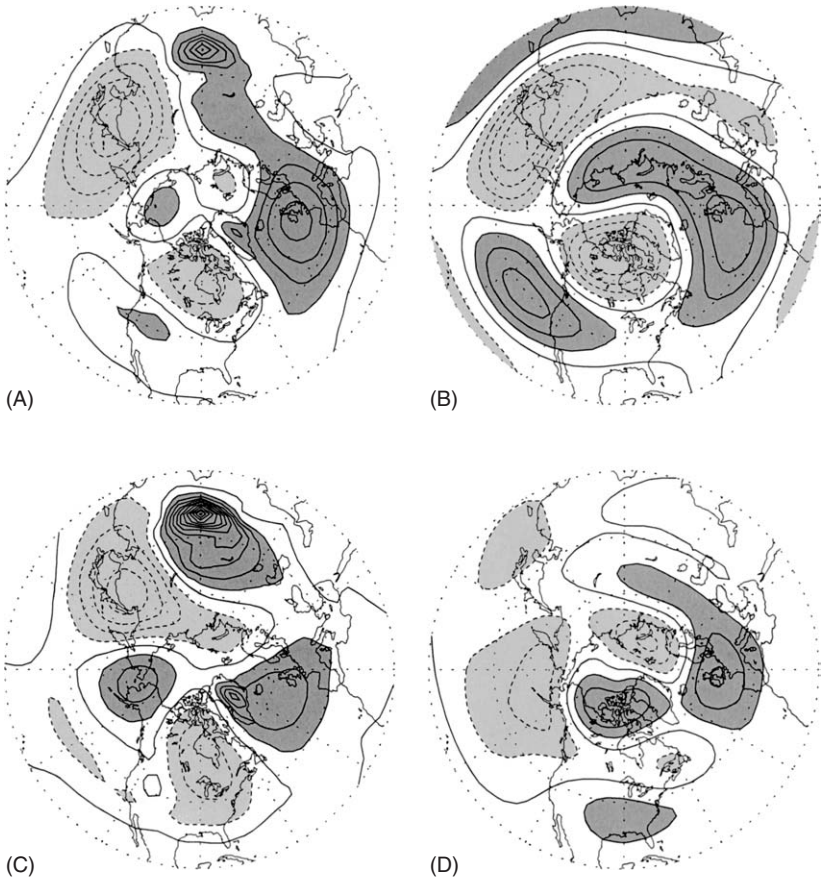

Figure 13 (A) The 300-hPa height response of a linear stationary wave model forced by heating, mountains, and transient fluxes of heat and momentum. The contour interval is 50 m, with dark (light) shading for positive (negative) values in excess of 50 m. (B–D) Response of the model when forced separately by (B) heating, (C) mountains, and (D) transient fluxes. The contour interval in (B–D) is 25 m.

forcing of the jets as well. The high amplitudes directly over Greenland and Tibet are a consequence of the linearization of the hydrostatic equation in σ-coordinates. Examination of geopotential heights gives a somewhat misleading impression that waves generated by mountains propagate primarily in the zonal direction. Examination of the modeled streamfunction (a more suitable variable for describing the rotational response in the tropics; not shown), however, reveals considerable equatorward propagation of the forced waves.

The forcing by submonthly transients (panel D) produces a somewhat intricate pattern with no clear relationship to the synoptic stormtracks. Transients are apparently responsible for a large part of the response over eastern Atlantic and northern Europe.

Studies of stationary wave dynamics have traditionally focused on the question of the relative importance of the various forcing terms in generating the observed pattern. Yet recent simulations such as the one in **Figure 13** show clearly that the northern winter stationary waves do not constitute a simple linear response to a single form of forcing. Furthermore, linearized equations, such as eqns [3] and [4], neglect the advection of eddy heat and vorticity by the stationary waves themselves, and also the effect of eddy winds impinging on the mountains. These terms play an important role in generating some features of the stationary wave pattern, such as the ridge over the Rockies. Future examinations of stationary wave dynamics will have to assess not only the relative importance of various forcing terms but their mutual interactions, and the nonlinear interactions of the stationary waves themselves.

See also

Climate Variability: Seasonal to Interannual Variability. **Coriolis Force**. **Cyclogenesis**. **Dynamic Meteorology:** Overview; Waves. **Stratosphere–Troposphere Exchange:** Global Aspects.

Further Reading

Gill AE (1982) *Atmosphere–Ocean Dynamics*. Orlando: Academic Press.

Grotjahn R (1993) *Global Atmospheric Circulations: Observations and Theories*. New York: Oxford University Press.

Holton JR (1992) *An Introduction to Dynamic Meteorology*. New York: Academic Press.

Hoskins BJ and Karoly DJ (1981) The steady linear response of a spherical atmosphere to thermal and orographic forcing. *Journal of the Atmospheric Sciences* 38: 1179–1196.

Hoskins BJ and Pearce R (1983) *Large-Scale Dynamical Processes in the Atmosphere*. London: Academic Press.

James IN (1994) *Introduction to Circulating Atmospheres*. Cambridge: Cambridge University Press.

Saltzman B and Manabe S (eds) (1985) *Advances in Geophysics*, vol. 28, *Issues in Atmospheric and Oceanic Modeling*. Orlando: Academic Press.

STRATOSPHERE–TROPOSPHERE EXCHANGE

Contents

Global Aspects

J R Holton, University of Washington, Seattle, WA, USA

Introduction

The troposphere and the stratosphere are separated by a boundary called the tropopause, whose altitude varies from about 16 km in the tropics to about 8 km near the poles. The troposphere is characterized by rapid vertical transport and mixing caused by weather disturbances; the stratosphere is characterized by very weak vertical transport and mixing. The tropopause thus represents a boundary between the troposphere, where chemical constituents tend to be well mixed, and the stratosphere, where chemical constituents tend to have strong vertical gradients. The two-way exchange of material that occurs across the tropopause is important for determining the climate and chemical composition of the upper troposphere and the lower stratosphere. This cross-tropopause